Magnetic breakdown and quantum oscillations in electron-doped high-temperature superconductor $Nd_{2-x}Ce_xCuO_4$

Jonghyoun Eun and Sudip Chakravarty

Department of Physics and Astronomy, University of California Los Angeles, Los Angeles, California 90095-1547, USA

(Received 8 July 2011; published 12 September 2011)

Recent, more precise experiments have revealed both a slow and a fast quantum oscillation in the c-axis resistivity of nearly optimal to overdoped electron-doped high-temperature superconductor $Nd_{2-x}Ce_xCuO_4$. Here, we study this problem from the perspective of Fermi surface reconstruction using an exact transfer matrix method and the Pichard-Landauer formula. In this method, neither quasiclassical approximations for magnetic breakdown nor *ad hoc* broadening of Landau levels is necessary to study the high-field quantum oscillations. The underlying Hamiltonian is a mean-field Hamiltonian that incorporates a twofold commensurate Fermi surface reconstruction. While the specific mean field considered is the d-density wave, similar results can also be obtained by a model of a spin density wave, as was explicitly demonstrated earlier. The results are consistent with an interplay of magnetic breakdown across small gaps in the reconstructed Fermi surface and Shubnikov–de Haas oscillations.

DOI: 10.1103/PhysRevB.84.094506 PACS number(s): 74.72.Ek, 74.25.Jb, 74.25.Ha, 74.20.−z

I. INTRODUCTION

Quantum oscillations were first discovered[1] in the Hall coefficient of a hole-doped high-temperature superconductor $YBa_2Cu_3O_{6+\delta}$ (YBCO) at high magnetic fields between 35 and 62 T in the underdoped regime close to 10%. Since then, a number of measurements, in even higher fields and with greater precision using a variety of measurement techniques, have confirmed the basic features of this experiment. However, the precise mechanism responsible for oscillations has become controversial.[2] Fermi surface reconstruction due to a density wave order that could arise if superconductivity is "effectively destroyed" by high magnetic fields has been the focus of some attention.[3]

In contrast, similar quantum oscillation measurements in the doping range 15–17% in $Nd_{2-x}Ce_xCuO_4$ (NCCO)[4] seem easier to interpret, as the magnetic field range 30–65 T is far above the upper critical field, which is less than 10 T. This clearly places the material in the "normal" state, a source of contention in measurements in YBCO; in NCCO, the crystal structure consists of a single CuO plane per unit cell, and, in contrast to YBCO, there are no complicating chains, bilayers, ortho-II potential, stripes, etc.[5] Thus, it would appear to be ideal for gleaning the mechanism of quantum oscillations. On the other hand, disorder in NCCO is significant. It is believed that well-ordered chain materials of YBCO contain much less disorder by comparison.

In a previous publication,[6] we mentioned in passing that it is not possible to understand the full picture in NCCO without magnetic breakdown effects, since the gaps are expected to be very small in the relevant regime of the parameter space. However, in that preliminary work, the breakdown phenomenon was not addressed; instead, we focused our attention on the effect of disorder. Since then, recent measurements[7,8] have indeed revealed magnetic breakdown in the range 16–17% doping, almost to the edge of the superconducting dome. Here, we consider the same transfer matrix method used previously,[6] but we include third-neighbor hopping of electrons on the square planar lattice, without which many experimental aspects cannot be faithfully reproduced, including quantitative estimates of the oscillation frequencies and breakdown effects. The third-neighbor hopping makes the numerical transfer matrix calculation more intensive because of the enlarged size of the matrix, but we were able to overcome the technical challenges. In this paper, we also analyze the c-axis resistivity and the absence of the electron pockets in the experimental regime.

II. HAMILTONIAN

The mean-field Hamiltonian for a d-density wave[9] (DDW) in real space, in terms of the site-based fermion annihilation and creation operators $c_{\mathbf{i}}$ and $c_{\mathbf{i}}^\dagger$, is

$$H_{\mathrm{DDW}} = \sum_{\mathbf{i}} \epsilon_{\mathbf{i}} c_{\mathbf{i}}^\dagger c_{\mathbf{i}} + \sum_{\mathbf{i},\mathbf{j}} t_{\mathbf{i},\mathbf{j}} e^{i a_{\mathbf{i},\mathbf{j}}} c_{\mathbf{i}}^\dagger c_{\mathbf{j}} + \mathrm{H.c.}, \tag{1}$$

where the nearest-neighbor hopping matrix elements include a DDW gap W_0 and are

$$\begin{aligned} t_{\mathbf{i},\mathbf{i}+\hat{\mathbf{x}}} &= -t + \tfrac{i W_0}{4}(-1)^{(n+m)}, \\ t_{\mathbf{i},\mathbf{i}+\hat{\mathbf{y}}} &= -t - \tfrac{i W_0}{4}(-1)^{(n+m)}, \end{aligned} \tag{2}$$

where (n,m) are a pair of integers labeling a site: $\mathbf{i} = n\hat{\mathbf{x}} + m\hat{\mathbf{y}}$; the lattice constant a will be set to unity unless otherwise specified. In this paper, we also include both the next-nearest-neighbor hopping matrix element, t', and the third-nearest-neighbor hopping matrix element, t''. A constant perpendicular magnetic field B is included via the Peierls phase factor $a_{\mathbf{i},\mathbf{j}} = \frac{e}{\hbar c}\int_{\mathbf{j}}^{\mathbf{i}} \mathbf{A}\cdot d\mathbf{l}$, where $\mathbf{A} = (0, -Bx, 0)$ is the vector potential in the Landau gauge. The band parameters are chosen to be $t = 0.38$ eV, $t' = 0.32t$, and $t'' = 0.5t'$.[10] The chemical potential μ is adjusted to achieve the required doping level and is given in Table I, as is the DDW gap W_0. We assume that the on-site energy is δ-correlated white noise defined by the disorder average $\overline{\epsilon_{\mathbf{i}}} = 0$ and $\overline{\epsilon_{\mathbf{i}}\epsilon_{\mathbf{j}}} = V_0^2\delta_{\mathbf{i},\mathbf{j}}$. Disorder levels for each of the cases studied are also given in Table I. The range of parameters chosen covered the estimates made in Ref. 8. We have seen previously that longer-ranged correlated disorder led to very similar results.[11]

TABLE I. Parameters W_0 (DDW gap), V_0 (on-site disorder potential), and μ (chemical potential).

Figure	Gap W_0 (meV)	μ	doping (%)
Fig. 2	5	$0.057t$	17
Fig. 3	10	$0.057t$	17
Fig. 4	15	$0.0176t$	16
Fig. 5	30	$0.0176t$	16

The Fermi surface areas (see Fig. 1) of the small hole pocket in the absence of disorder correspond to oscillation frequencies 330 T at 15% doping, 317 T at 16% doping, and 291 T at 17% doping. These frequencies seem to be insensitive to W_0 within the range given in Table I.

III. THE TRANSFER MATRIX METHOD

The transfer matrix to compute the oscillations of the conductance is a powerful method. It requires neither a quasiclassical approximation to investigate magnetic breakdown nor *ad hoc* broadening of the Landau level to incorporate the effect of disorder. Various models of disorder, both long- and short-ranged, can be studied *ab initio*. The mean-field Hamiltonian, being a quadratic noninteracting Hamiltonian, leads to a Schrödinger equation for the site amplitudes, which is then recast in the form of a transfer matrix; the full derivation is given in the Appendix. The conductance is then calculated by a formula that is well known in the area of mesoscopic physics, namely the Pichard-Landauer formula.[12] This yields Shubnikov–de Haas oscillations of the ab-plane resistivity, ρ_{ab}. We show later how this can be related to the c-axis resistivity ρ_c measured in experiments.

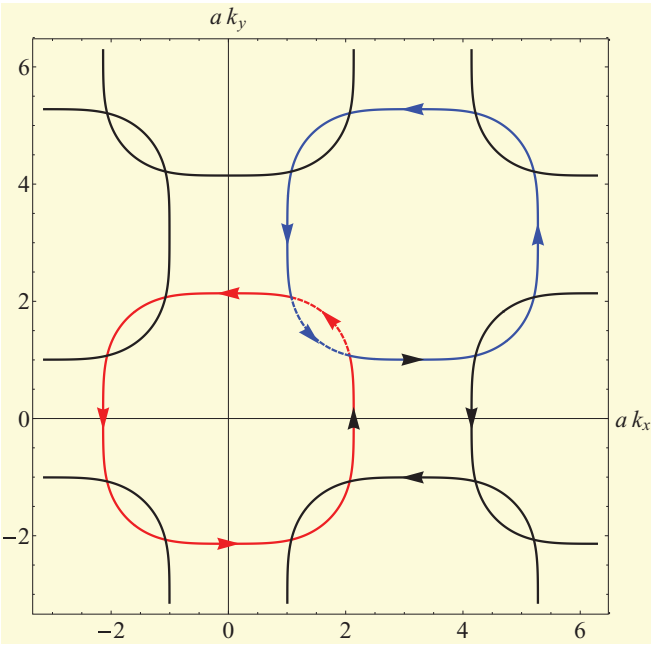

FIG. 1. (Color online) A plot showing the breakdown junctions and electron trajectories across them in the extended Brillouin zone. The figure corresponds to NCCO with 17% doping and a small DDW gap. Note that the reflection at the junctions involves a large change in momentum. The electron trajectories that lead to magnetic breakdown of small hole pockets are shown.

Consider a quasi-1D system, $N \gg M$, with a periodic boundary condition along the y direction. Here, Na is the length in the x direction and Ma is the length in the y direction, a being the lattice spacing. Let $\Psi_n = (\psi_{n,1}, \psi_{n,2}, \ldots, \psi_{n,M})^T$, $n = 1, \ldots, N$, be the amplitudes on the slice n for an eigenstate with a given energy. Then the amplitudes on four successive slices must satisfy the relation

$$\begin{bmatrix} \Psi_{n+2} \\ \Psi_{n+1} \\ \Psi_n \\ \Psi_{n-1} \end{bmatrix} = \begin{bmatrix} U_n^{-1}A_n & U_n^{-1}B_n & U_n^{-1}C_n & U_n^{-1}D_n \\ 1 & 0 & 0 & 0 \\ 0 & 1 & 0 & 0 \\ 0 & 0 & 1 & 0 \end{bmatrix} \begin{bmatrix} \Psi_{n+1} \\ \Psi_n \\ \Psi_{n-1} \\ \Psi_{n-2} \end{bmatrix}$$

$$= \mathbf{T}_n \begin{bmatrix} \Psi_{n+1} \\ \Psi_n \\ \Psi_{n-1} \\ \Psi_{n-2} \end{bmatrix}, \tag{3}$$

where U_n, A_n, B_n, C_n, and D_n are $M \times M$ matrices. The nonzero matrix elements of matrix A_n are

$$(A_n)_{m,m} = -\left[-1 - \frac{iW_0}{4}(-1)^{m+n}\right], \tag{4}$$

$$(A_n)_{m,m+1} = -t' e^{i(-n-\frac{1}{2})\phi}, \tag{5}$$

$$(A_n)_{m,m-1} = -t' e^{i(n+\frac{1}{2})\phi}, \tag{6}$$

where $\phi = Ba^2e/\hbar c$ is a constant. The elements of the matrix B_n are

$$(B_n)_{m,m} = \epsilon_{n,m} - \mu, \tag{7}$$

$$(B_n)_{m,m+1} = \left[-1 + \frac{iW_0}{4}(-1)^{m+n}\right] e^{-in\phi}, \tag{8}$$

$$(B_n)_{m,m-1} = \left[-1 + \frac{iW_0}{4}(-1)^{m+n}\right] e^{in\phi}, \tag{9}$$

$$(B_n)_{m,m+2} = t'' e^{-i2n\phi}, \tag{10}$$

$$(B_n)_{m,m-2} = t'' e^{i2n\phi}. \tag{11}$$

Here $C_n = A_n^\dagger$ and $D_n = -U_n = t''\mathbb{1}$, where $\mathbb{1}$ is the $M \times M$ identity matrix.

The $4M$ Lyapunov exponents, γ_i, of $\lim_{N\to\infty}(\mathcal{T}_N\mathcal{T}_N^\dagger)$, where $\mathcal{T}_N = \prod_{j=1}^{j=N} \mathbf{T}_j$, are defined by the corresponding eigenvalues $\lambda_i = e^{\gamma_i}$. All the Lyapunov exponents $\gamma_1 > \gamma_2 > \cdots > \gamma_{4M}$, are computed by a method described in Ref. 13. However, the matrix is not symplectic. Therefore, all $4M$ eigenvalues are computed. Remarkably, except for a small set consisting of large eigenvalues, the rest of the eigenvalues do come in pairs $(\lambda, 1/\lambda)$, as for the symplectic case, within our numerical accuracy. We have no analytical proof of this curious fact. Clearly, large eigenvalues contribute insignificantly to the Pichard-Landauer[12] formula for the conductance, $\sigma_{ab}(B)$:

$$\sigma_{ab}(B) = \frac{e^2}{h}\mathrm{Tr}\sum_{j=1}^{2M} \frac{2}{(\mathcal{T}_N\mathcal{T}_N^\dagger) + (\mathcal{T}_N\mathcal{T}_N^\dagger)^{-1} + 2}. \tag{12}$$

We have chosen M to be 32, smaller than our previous work.[6] The reason for this is that the matrix size including the third-neighbor hopping is larger, $4M \times 4M$ instead of $2M \times 2M$.

We chose N to be of the order of 10^6, as before. This easily led to an accuracy better than 5% for the smallest Lyapunov exponent, γ_i, in all cases.

IV. MAGNETIC BREAKDOWN AND QUANTUM OSCILLATIONS

We compute the conductance as a function of the magnetic field and then Fourier transform the numerical data. This procedure depends of course on the number of data points sampled within a fixed range of the magnetic field, typically between 45 and 60 T. But the location of each peak and the relative ratio of the intensities remain the same. In order to compare the Fourier transformed results, we keep the sampling points fixed in all cases to be 1200.

In Fig. 2, the results for 17% doping for a 5 meV gap and varying degrees of disorder are shown. Both the slow oscillation at a frequency 290 T corresponding to the small hole pocket and 11 700 T corresponding to the large hole pocket, as schematically sketched in Fig. 1 in the extended Brillouin zone, can be seen. Note that partitioning of the spectral weight between the peaks changes as the degree of disorder is increased. If we change the value of the gap to 10 meV, shown in Fig. 3, the overall picture remains the same, although the lower frequency peak is a bit more dominant, as the magnetic breakdown is a little less probable.

For 16% doping, a similar calculation with gaps of 15 and 30 meV also shows some evidence of magnetic breakdown depending on the disorder level, particularly seen in the 15 meV data in Fig. 4. On the other hand, the evidence of magnetic breakdown is much weaker in the 30 meV data shown in Fig. 5. It is important to note that in none of these calculations does one find any evidence of the electron pocket centered at $(\pi,0)$ and its symmetry counterparts, which should correspond roughly to a frequency of 2700 T. This is due in part to the fact that the effect of disorder is stronger on the electron pocket[6] and in part to the fact that at the breakdown junctions transmission coefficient is larger than the reflection coefficient because it entails a large $(\pi/2)$ change in the direction of the momentum; see Fig. 1.

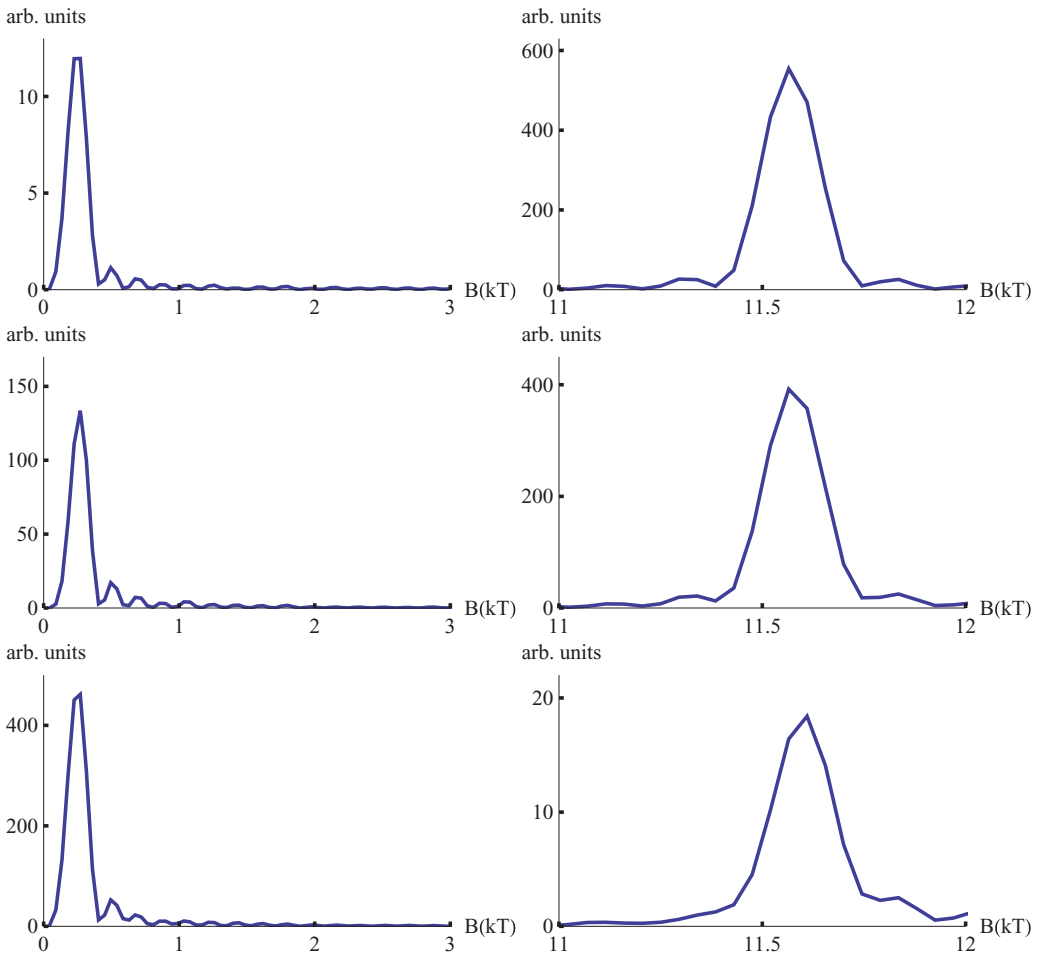

FIG. 2. (Color online) Fourier transform of the conductance oscillations with a smooth background term subtracted. The parameters correspond to 17% doping with a DDW gap of 5 meV and disorder $V_0 = 0.2t$ (row 1), $V_0 = 0.4t$ (row 2), and $V_0 = 0.6t$ (row 3). The horizontal axis is a magnetic field in terms of kilo-Tesla (10^3 T) and the vertical axis is in arbitrary units. The left panels in all cases show the lower frequency component and the right panel the higher-frequency component. Note that there is no evidence of the electron pocket frequency at about $B = 2.7$ kT.

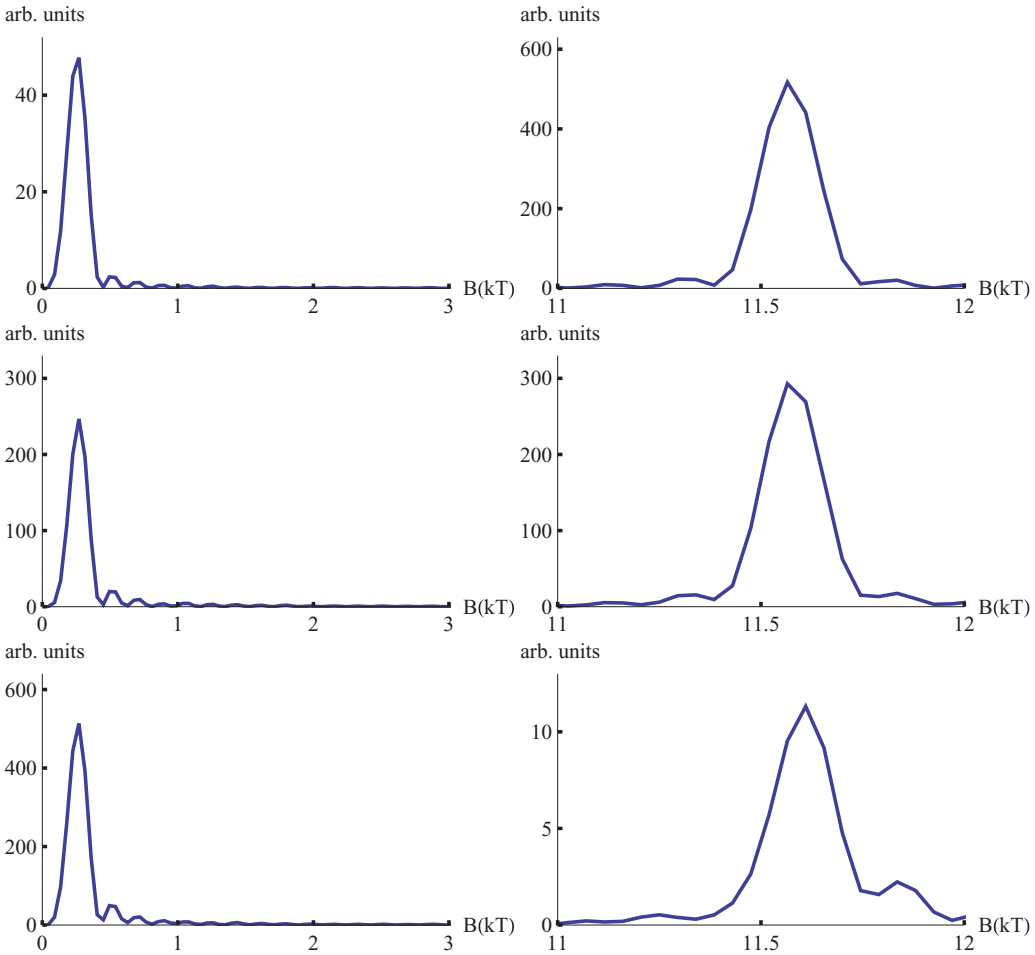

FIG. 3. (Color online) Fourier transform of the conductance oscillations with a smooth background term subtracted. The parameters correspond to 17% doping with a DDW gap of 10 meV and disorder $V_0 = 0.2t$ (row 1), $V_0 = 0.4t$ (row 2), and $V_0 = 0.6t$ (row 3). The horizontal axis is a magnetic field in terms of kilo-Tesla (10^3 T) and the vertical axis is in arbitrary units. The left panels in all cases show the lower frequency component and the right panel the higher frequency component. Note that there is no evidence of the electron pocket frequency at about $B = 2.7$ kT.

V. OSCILLATIONS IN *c*-AXIS RESISTIVITY

The Pichard-Landauer formula was calculated for conductance oscillations in the ab plane, while the actual measurements in NCCO are carried out for the c-axis resistivity. It is therefore necessary to relate the two to compare with experiments. A simple description for a strongly layered material can be obtained by modifying an argument of Kumar and Jayannavar.[14] An applied electric field, E, along the direction perpendicular to the planes will result in a chemical potential difference

$$\Delta\mu = edE, \tag{13}$$

where d is the distance between the two planes of a unit cell. The corresponding current, j_c, is (ε_F is the Fermi energy)

$$j_c = e\,[\Delta\mu g_{2D}(\varepsilon_F, H)]\,\gamma, \tag{14}$$

since $\Delta\mu g_{2D}(\varepsilon_F, H)$ is the number of unoccupied states to which an electron can scatter, while γ is the scattering rate between the planes of a unit cell. Here, we have included a possible oscillatory dependence of the the two-dimensional density of states, $g_{2D}(\varepsilon_F, H)$, that gives rise to Shubnikov–de Haas oscillations in the ab plane. Thus,

$$\rho_c = \frac{E}{j_c} = \frac{1}{e^2 d g_{2D}(\varepsilon_F)\gamma}. \tag{15}$$

There is an implicit assumption: an electron from a given plane makes a transition to a continuum of available states with a finite density at the Fermi surface in the next plane. We are not interested in the Rabi oscillations between two discrete states, a process that cannot lead to resistivity.

The measured ab-plane resistivity is of the order 10 $\mu\Omega$ cm as compared to Ω cm for the c-axis resistivity even at optimum doping,[5] which allows us to make an adiabatic approximation. Because an electron spends much of its time in the plane, making only infrequent hops between the planes, we can adiabatically decouple these two processes. The slower motion along the c axis can be formulated in terms of a 2×2 matrix for each parallel wave vector $\mathbf{k}_\parallel$ after integrating out the planar modes. For simplicity, we are assuming that the c-axis warping is negligible, so there are only two available states of the electron corresponding to its locations in the two planes. The excitations in a plane close to the Fermi surface, $k_\parallel \approx k_{F,\parallel}$, can be approximated by a bosonic heat bath of

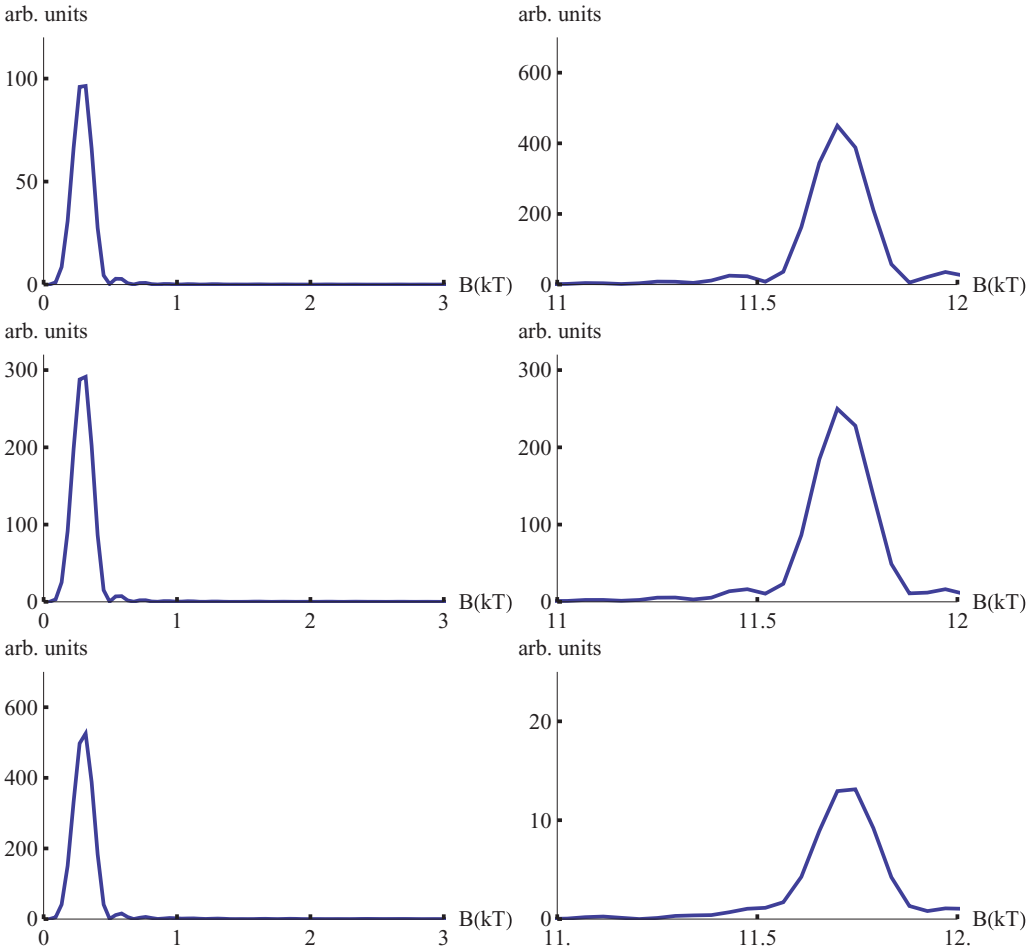

FIG. 4. (Color online) Fourier transform of the conductance oscillations with a smooth background term subtracted. The parameters correspond to 16% doping with a DDW gap of 15 meV and disorder $V_0 = 0.2t$ (row 1), $V_0 = 0.4t$ (row 2), and $V_0 = 0.6t$ (row 3). The horizontal axis is a magnetic field in terms of kilo-Tesla (10^3 T) and the vertical axis is in arbitrary units. The left panels in all cases show the lower frequency component and the right panel the higher frequency component. Note that there is no evidence of the electron pocket frequency at about $B = 2.7$ kT.

particle-hole excitations. In this language, the problem maps onto a two-state Hamiltonian,

$$H = -t_c\sigma_x + \sum_j \hbar\omega_j b_j^\dagger b_j + \frac{\sigma_z}{2}\sum_j f_j(b_j^\dagger + b_j), \qquad (16)$$

where σ's are the standard Pauli matrices and t_c is the hopping matrix element between the nearest-neighbor planes. Given the simplification, the sum over $\mathbf{k}_\parallel$ is superfluous, and the problem then maps onto a much studied model of a two-level system coupled to an Ohmic heat bath.[15] The Ohmic nature follows from the fermionic nature of the bath.[16] The effect of the bath on the transition between the planes is summarized by a spectral function,

$$J(\omega) = \frac{\pi}{2}\sum_j f_j^2\delta(\omega - \omega_j). \qquad (17)$$

For a fermionic bath, we can choose

$$J(\omega) = \begin{cases} 2\pi\alpha\omega, & \omega \ll \omega_c \\ 0, & \omega \gg \omega_c, \end{cases} \qquad (18)$$

where ω_c is a high-frequency cutoff, which is of the order of $\omega_c = 2/\tau_{ab}$, where τ_{ab} is of the order of the planar relaxation time. For a Fermi bath, the parameter α is necessarily restricted to the range $0 \leqslant \alpha \leqslant 1$.[16] Moreover, for coherent oscillations we must have $\alpha < 1/2$.[15] However, we shall leave α as an adjustable parameter, presumably less than or equal to $1/2$ to be consistent with our initial assumptions. While a similar treatment is possible for a non-Fermi liquid,[17] the present discussion is entirely within the Fermi liquid theory.

The quantity γ is the interplanar tunneling rate renormalized by the particle-hole excitations close to the planar Fermi surface and can be easily seen to be[15]

$$\gamma = \frac{2t_c}{\hbar}\left(\frac{2t_c}{\hbar\omega_c}\right)^{\frac{\alpha}{1-\alpha}}. \qquad (19)$$

The c-axis resistivity is then

$$\rho_c = \frac{\hbar}{e^2}\frac{1}{d g_{2D}(\varepsilon_F, H)\hbar\omega_c}\left(\frac{\hbar\omega_c}{2t_c}\right)^{\frac{1}{1-\alpha}}. \qquad (20)$$

This equation can be further simplified by expressing it as a ratio of ρ_c/ρ_{ab}, but this is unnecessary. Two important qualitative points are as follows: ρ_c is far greater than ρ_{ab},

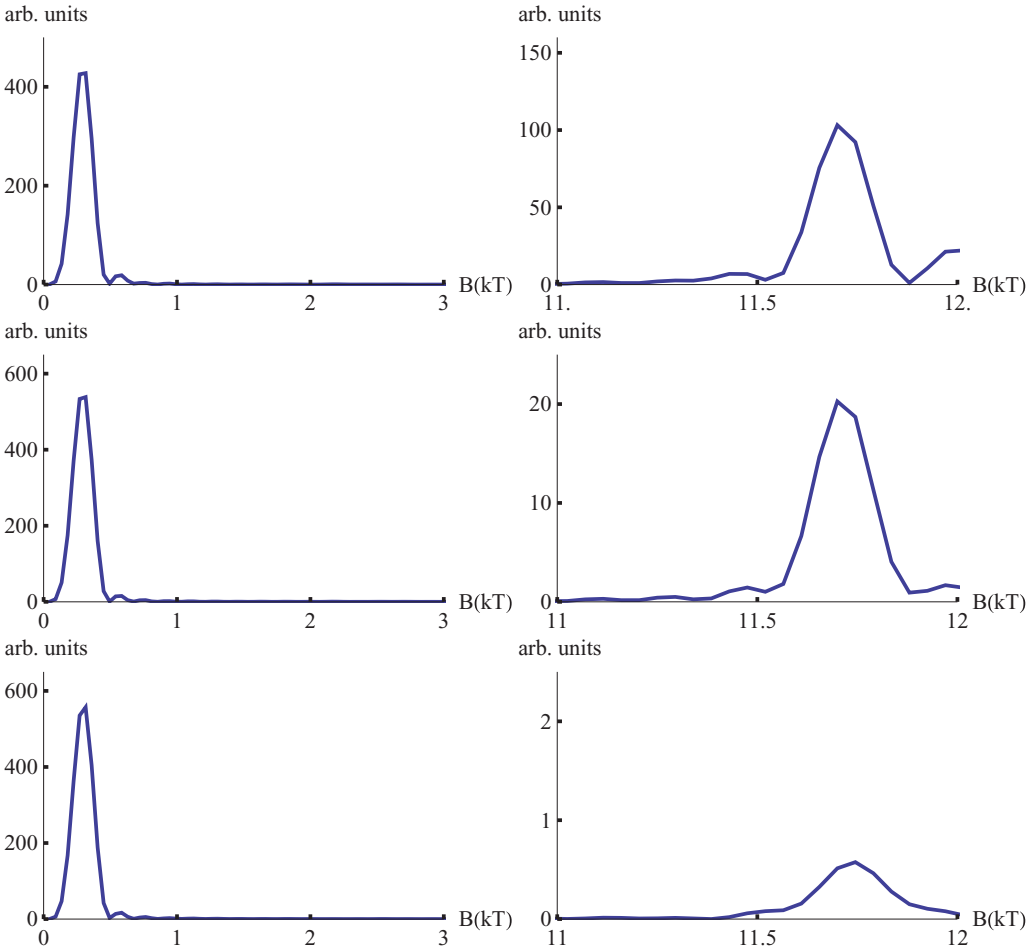

FIG. 5. (Color online) Fourier transform of the conductance oscillations with a smooth background term subtracted. The parameters correspond to 16% doping with a DDW gap of 30 meV and disorder $V_0 = 0.2t$ (row 1), $V_0 = 0.4t$ (row 2), and $V_0 = 0.6t$ (row 3). The horizontal axis is a magnetic field in terms of kilo-Tesla (10^3 T) and the vertical axis is in arbitrary units. The left panels in all cases show the lower frequency component and the right panel the higher frequency component. Note that there is no evidence of the electron pocket frequency at about $B = 2.7$ kT.

and the root of the quantum oscillations of ρ_c is quantum oscillations of the planar density of states.

VI. CONCLUSIONS

We have shown that a qualitatively consistent physical picture for quantum oscillations can be provided with a simple set of assumptions involving reconstruction of the Fermi surface due to density wave order. Although not presented here, we have also noted that even for 15% doping one can observe magnetic breakdown if the gap is small, in the range 20–30 meV. This appears to be consistent with even more recent unpublished experiments.[18] Although the specific order considered here was the DDW, we have shown previously that at the mean-field level, a very similar picture can be provided by a twofold commensurate spin density wave (SDW).[6] Thus, it appeared unnecessary to repeat the same calculations using the SDW order.

In YBCO, studies involving tilted fields seem to rule out a triplet order parameter, hence the SDW.[19] Moreover, from nuclear magnetic resonance (NMR) measurements at high fields, there appears to be no evidence of a static spin density wave order in YBCO.[20] Similarly, there is no evidence of SDW order in fields as high as 23.2 T in $YBa_2Cu_4O_8$,[21] while quantum oscillations are clearly observed in this material.[22] Also, no such evidence of SDW is found up to 44 T in $Bi_2Sr_{2-x}La_xCuO_{6+\delta}$.[23] At present, results from high-field NMR in NCCO do not exist, but measurements are in progress.[24] It is unlikely that such static SDW order will be revealed in these measurements. This conjecture is based on the zero-field neutron-scattering measurements, which indicate a very small spin-spin correlation length in the relevant doping regime.[25] A long-range SDW order cannot appear merely by applying high magnetic fields, which is energetically a weak perturbation even for a 45 T field.[26]

As to singlet order, most likely relevant to the observation of quantum oscillations,[27] a charge density wave is a possibility. This has recently found some support in the high-field NMR measurements in YBCO.[20] As to singlet DDW, there are two neutron scattering measurements that seem to provide evidence for it.[28] However, these measurements have not been confirmed by further independent experiments. However, DDW order should be considerably hidden in NMR involving nuclei at high symmetry points, because the orbital currents should cancel.

A mysterious feature of quantum oscillations in YBCO is the fact that only one type of Fermi pocket is observed. If a twofold commensurate density wave is the mechanism, this will violate the Luttinger sum rule.[3,29] We have previously provided an explanation for this phenomenon in terms of disorder arising from both defects and vortex scattering in the vortex liquid phase.[11] However, the arguments are not unassailable. In contrast, for NCCO, the experimental results are quite consistent with the simple theory discussed above. We have not addressed angle-dependent magnetoresistance oscillations (AMRO) in NCCO, as the data seem to be somewhat anomalous,[8] although within the Fermi liquid framework discussed here it should be possible to address this effect in the future.

The basic question as to why Fermi liquid concepts should apply remains an important unsolved mystery.[30] It is possible that if the state revealed by applying a high magnetic field has a broken symmetry with an order parameter (hence a gap), the low-energy excitations will be quasiparticle-like, not spectra with a branch cut, as in variously proposed strange metal phases. In this respect, the notion of a hidden Fermi liquid may be relevant.[31]

ACKNOWLEDGMENTS

We thank Mark Kartsovnik, Stuart Brown, Marc-Henri Julien, Brad Ramshaw, and Cyril Proust for keeping us updated regarding their latest experiments. In particular, we thank Marc-Henri Julien for sharing with us his unpublished high-field NMR results in YBCO. This work is supported by the NSF under Grant No. DMR-1004520.

APPENDIX: THE DERIVATION OF THE TRANSFER MATRIX

The DDW Hamiltonian in real space is

$$H=\sum_{\mathbf{i}}\epsilon_{\mathbf{i}}c_{\mathbf{i}}^{\dagger}c_{\mathbf{i}}-t\sum_{\langle\mathbf{i},\mathbf{j}\rangle}e^{ia_{\mathbf{i},\mathbf{j}}}c_{\mathbf{i}}^{\dagger}c_{\mathbf{j}}-t'\sum_{\langle\mathbf{i},\mathbf{j}\rangle'}e^{ia_{\mathbf{i},\mathbf{j}}}c_{\mathbf{i}}^{\dagger}c_{\mathbf{j}}-t''\sum_{\langle\mathbf{i},\mathbf{j}\rangle''}e^{ia_{\mathbf{i},\mathbf{j}}}c_{\mathbf{i}}^{\dagger}c_{\mathbf{j}}+\sum_{\mathbf{i}}\frac{iW_0}{4}(-1)^{n+m}c_{\mathbf{i}}^{\dagger}c_{\mathbf{i}+\hat{\mathbf{x}}}-\sum_{\mathbf{i}}\frac{iW_0}{4}(-1)^{n+m}c_{\mathbf{i}}^{\dagger}c_{\mathbf{i}+\hat{\mathbf{y}}}+\text{H.c.} \tag{A1}$$

Here, $e^{ia_{\mathbf{i},\mathbf{j}}}$ is the Peierls phase due to the magnetic field. The summation notations are as follows: $\langle\mathbf{i},\mathbf{j}\rangle$, $\langle\mathbf{i},\mathbf{j}\rangle'$, and $\langle\mathbf{i},\mathbf{j}\rangle''$ imply a sum over nearest-neighbor, next-nearest-neighbor, and the third-nearest-neighbor sites, respectively. For example, with the lattice constant set to unity, $\langle\mathbf{i},\mathbf{j}\rangle$ is satisfied when $\mathbf{i}=\mathbf{j}\pm\hat{\mathbf{x}}$ or $\mathbf{i}=\mathbf{j}\pm\hat{\mathbf{y}}$. Likewise, $\langle\mathbf{i},\mathbf{j}\rangle'$ requires $\mathbf{i}=\mathbf{j}+\hat{\mathbf{x}}\pm\hat{\mathbf{y}}$ or $\mathbf{i}=\mathbf{j}-\hat{\mathbf{x}}\pm\hat{\mathbf{y}}$ and $\langle\mathbf{i},\mathbf{j}\rangle''$ requires $\mathbf{i}=\mathbf{j}\pm2\hat{\mathbf{x}}$ or $\mathbf{i}=\mathbf{j}\pm2\hat{\mathbf{y}}$. Here W_0 is the DDW gap and $\mathbf{i}=(n,m)$. Consider an eigenstate $|\Psi\rangle$ with an energy eigenvalue E: $H|\Psi\rangle=E|\Psi\rangle$, where $|\Psi\rangle=\sum_{\mathbf{i}}\psi(\mathbf{i})|\mathbf{i}\rangle$; the amplitude at a site is $\psi(\mathbf{i})$. Then the Schrödinger equation can be written in terms of the amplitudes $\psi_n(m)$ of the nth slice for all values of $m=1,2,\ldots,M$:

$$\begin{aligned}E\psi_n(m)=\epsilon_{\mathbf{i}}\psi_n(m)&-t[\psi_{n+1}(m)+\psi_{n-1}(m)+e^{-in\phi}\psi_n(m+1)\\&+e^{in\phi}\psi_n(m-1)]-t'[e^{i(-n-\frac{1}{2})\phi}\psi_{n+1}(m+1)\\&+e^{i(n+\frac{1}{2})\phi}\psi_{n-1}(m+1)+e^{i(n+\frac{1}{2})\phi}\psi_{n+1}(m-1)\\&+e^{i(-n-\frac{1}{2})\phi}\psi_{n-1}(m-1)]-t''[\psi_{n+2}(m)+\psi_{n-2}(m)\\&+e^{-i2n\phi}\psi_n(m+2)+e^{i2n\phi}\psi_n(m-2)]\\&+\frac{iW_0}{4}(-1)^{n+m}[\psi_{n+1}(m)+\psi_{n-1}(m)]\\&-\frac{iW_0}{4}(-1)^{n+m}[e^{-in\phi}\psi_n(m+1)+e^{in\phi}\psi_n(m-1)].\end{aligned} \tag{A2}$$

With the periodic boundary condition along the y axis, i.e., $\psi_n(M+1)=\psi_n(1)$, the Schrödinger equation can be expressed as a matrix equation:

$$0=-U_n\psi_{n+2}+A_n\psi_{n+1}+B_n\psi_n+C_n\psi_{n-1}+D_n\psi_{n-2}, \tag{A3}$$

where U_n, A_n, B_n, C_n, and D_n are $M\times M$ matrices defined in the equations following Eq. (3). Now we can solve the Schrödinger equation for ψ_{n+2} to obtain $\psi_{n+2}=U_n^{-1}(A_n\psi_{n+1}+B_n\psi_n+C_n\psi_{n-1}+D_n\psi_{n-2})$. Then the amplitudes at a set of four successive slices, ψ_{n-1} through ψ_{n+2}, can be written in terms of the amplitudes of a previous set of four successive slices, ψ_{n-2} through ψ_{n+1}. Thus, the transfer matrix in the main text follows.

[1] N. Doiron-Leyraud, C. Proust, D. LeBoeuf, J. Levallois, J.-B. Bonnemaison, R. Liang, D. A. Bonn, W. N. Hardy, and L. Taillefer, Nature (London) **447**, 565 (2007).

[2] S. C. Riggs, O. Vafek, J. B. Kemper, J. Betts, A. Migliori, W. N. Hardy, R. Liang, D. A. Bonn, and G. Boebinger, Nat. Phys. **7**, 332 (2011).

[3] S. Chakravarty, Science **319**, 735 (2008); S. Chakravarty and H.-Y. Kee, Proc. Natl. Acad. Sci. USA **105**, 8835 (2008); I. Dimov, P. Goswami, X. Jia, and S. Chakravarty, Phys. Rev. B **78**, 134529 (2008); A. J. Millis and M. R. Norman, *ibid.* **76**, 220503 (2007); H. Yao, D.-H. Lee, and S. A. Kivelson, Phys. Rev. B **84**, 012507 (2011).

[4] T. Helm, M. V. Kartsovnik, M. Bartkowiak, N. Bittner, M. Lambacher, A. Erb, J. Wosnitza, and R. Gross, Phys. Rev. Lett. **103**, 157002 (2009).

[5] N. P. Armitage, P. Fournier, and R. L. Green, Rev. Mod. Phys. **82**, 2421 (2009).

[6] J. Eun, X. Jia, and S. Chakravarty, Phys. Rev. B **82**, 094515 (2010).

[7] T. Helm, M. V. Kartsovnik, I. Sheikin, M. Bartkowiak, F. Wolff-Fabris, N. Bittner, W. Biberacher, M. Lambacher, A. Erb, J. Wosnitza, and R. Gross, Phys. Rev. Lett. **105**, 247002 (2010).

[8] M. V. Kartsovnik *et al.*, New J. Phys. **13**, 015001 (2011).

[9] S. Chakravarty, R. B. Laughlin, D. K. Morr, and C. Nayak, Phys. Rev. B **63**, 094503 (2001).

[10]E. Pavarini, I. Dasgupta, T. Saha-Dasgupta, O. Jepsen, and O. K. Andersen, Phys. Rev. Lett. **87**, 047003 (2001).
[11]X. Jia, P. Goswami, and S. Chakravarty, Phys. Rev. B **80**, 134503 (2009).
[12]J. L. Pichard and G. André, Europhys. Lett. **2**, 477 (1986); D. S. Fisher and P. A. Lee, Phys. Rev. B **23**, 6851 (1981).
[13]B. Kramer and M. Schreiber, in *Computational Physics*, edited by K. H. Hoffmann and M. Schreiber (Springer, Berlin, 1996), p. 166.
[14]N. Kumar and A. M. Jayannavar, Phys. Rev. B **45**, 5001 (1992).
[15]S. Chakravarty and A. J. Leggett, Phys. Rev. Lett. **52**, 5 (1984); A. J. Leggett, S. Chakravarty, A. T. Dorsey, M. P. A. Fisher, A. Garg, and W. Zwerger, Rev. Mod. Phys. **59**, 1 (1987).
[16]L.-D. Chang and S. Chakravarty, Phys. Rev. B **31**, 154 (1985).
[17]S. Chakravarty and P. W. Anderson, Phys. Rev. Lett. **72**, 3859 (1994).
[18]M. V. Kartsovnik (unpublished).
[19]B. J. Ramshaw, B. Vignolle, R. Liang, W. N. Hardy, C. Proust, and D. A. Bonn, Nat. Phys. **7**, 234 (2011); S. E. Sebastian, N. Harrison, M. M. Altarawneh, F. F. Balakirev, C. H. Mielke, R. Liang, D. A. Bonn, W. N. Hardy, and G. G. Lonzarich, e-print arXiv:1103.4178v1 (cond-mat).
[20]T. Wu, H. Mayaffre, S. Kramer, M. Horvatic, C. Berthier, W. Hardy, R. Liang, D. Bonn, and M.-H. Julien (unpublished).
[21]G.-q. Zheng, W. G. Clark, Y. Kitaoka, K. Asayama, Y. Kodama, P. Kuhns, and W. G. Moulton, Phys. Rev. B **60**, R9947 (1999).
[22]E. A. Yelland, J. Singleton, C. H. Mielke, N. Harrison, F. F. Balakirev, B. Dabrowski, and J. R. Cooper, Phys. Rev. Lett. **100**, 047003 (2008); A. F. Bangura, J. D. Fletcher, A. Carrington, J. Levallois, M. Nardone, B. Vignolle, P. J. Heard, N. Doiron-Leyraud, D. LeBoeuf, L. Taillefer, S. Adachi, C. Proust, and N. E. Hussey, *ibid*. **100**, 047004 (2008).
[23]S. Kawasaki, C. Lin, P. L. Kuhns, A. P. Reyes, and G.-q. Zheng, Phys. Rev. Lett. **105**, 137002 (2010).
[24]S. E. Brown (unpublished).
[25]E. M. Motoyama, G. Yu, I. M. Vishik, O. P. Vajk, P. K. Mang, and M. Greven, Nature (London) **445**, 186 (2007).
[26]H. K. Nguyen and S. Chakravarty, Phys. Rev. B **65**, 180519 (2002).
[27]D. Garcia-Aldea and S. Chakravarty, Phys. Rev. B **82**, 184526 (2010); M. R. Norman and J. Lin, *ibid*. **82**, 060509 (2010); R. Ramazashvili, Phys. Rev. Lett. **105**, 216404 (2010).
[28]H. A. Mook, P. Dai, S. M. Hayden, A. Hiess, J. W. Lynn, S. H. Lee, and F. Doğan, Phys. Rev. B **66**, 144513 (2002); H. A. Mook, P. Dai, S. M. Hayden, A. Hiess, S. H. Lee, and F. Doğan, *ibid*. **69**, 134509 (2004).
[29]J. M. Luttinger, Phys. Rev. **119**, 1153 (1960); A. V. Chubukov and D. K. Morr, Phys. Rep. **288**, 355 (1997); B. L. Altshuler, A. V. Chubukov, A. Dashevskii, A. M. Finkel'stein, and D. K. Morr, Europhys. Lett. **41**, 401 (1998).
[30]S. Chakravarty, Rep. Prog. Phys. **74**, 022501 (2011).
[31]P. A. Casey and P. W. Anderson, Phys. Rev. Lett. **106**, 097002 (2011).